



## Comparison of nickel release and cytocompatibility between porous and dense NiTi alloy

Ben-quan YU<sup>1</sup>, Wen-hui YUAN<sup>1</sup>, Qiang XU<sup>2</sup>, Yun-fang-zi GU<sup>1</sup>,  
Ming-ming XIAO<sup>1</sup>, Guo-fu XU<sup>2</sup>, Zhou LI<sup>2</sup>, Zhu XIAO<sup>2</sup>, Zi-an XIAO<sup>1</sup>

1. Department of Otolaryngology Head and Neck Surgery of Second Xiangya Hospital, Central South University, Changsha 410011, China;
2. School of Materials Science and Engineering, Central South University, Changsha 410083, China

Received 9 January 2021; accepted 25 August 2021

**Abstract:** The porous NiTi (pNiTi) samples were produced by sintering evaporation using Ti–50.8Ni (at.%) gas-atomized powders. The samples were analyzed by metallographic microscope and X-ray dispersive spectroscopy (XRD). A comparison of nickel (Ni) release and cytocompatibility between pNiTi and dense NiTi (dNiTi) was made. The results showed that the pNiTi has good mechanical properties. Ni releases from pNiTi in vitro and in vivo are more serious than those from dNiTi. The proliferation and differentiation of cells cultured with the pNiTi extracting liquid are significantly worse, and the rate of early apoptosis is higher. In conclusion, pNiTi is mechanically similar to bone, but pNiTi releases more Ni and interferes with cell proliferation and differentiation. A significantly cautious approach should be adopted when using it as a medical implant.

**Key words:** porous nitinol alloy; mechanical property; nickel release; cytocompatibility

### 1 Introduction

Nitinol (NiTi) shape memory alloy has been extensively used for decades in bone tissue engineering, stents, dental and orthopedic implants; this is because of its unique functional properties, specifically the shape memory effect, super-elasticity, damping capacity, satisfactory biocompatibility and biomechanics [1–3]. Notably, the elastic modulus of dense NiTi (dNiTi) alloy is between 40 and 75 GPa based on its transformation temperature and crystallographic texture [4]. Normally, the elastic modulus of cortical bone is between 17 and 20 GPa, whereas that of cancellous bone is approximately 1.15 GPa [5,6]. The mismatch of elastic modulus between the implant and the surrounding bone causes stress shielding,

i.e., the slow healing and reduction of bone density. Stress shielding is minimized by using implant materials with the elastic modulus close to that of the surrounding bone.

Porous metal is a typical functional material with specific properties. For instance, by increasing the sintering temperature, the porosities of the porous NiTi (pNiTi) gradually decrease and the compressive strength increases first, reaching a maximum value at 900 °C, and then decreases [7]. Thus, pNiTi resolves the stress shielding by changing its porosity to adjust the engineering elastic modulus and match that of the cortical bone [5]. The unique bone-like properties of low stiffness and superelastic behavior make them promising for biomedical applications [8]. Besides lowering the effective elastic modulus, pNiTi dramatically improves bony ingrowth and surface

friction. Notably, in vivo and in vitro experiments have confirmed its efficient biocompatibility [9]. Nevertheless, the complex body environment may introduce challenges of implant corrosion and nickel (Ni) release control [10]. In our previous work [11], we found a tiny amount of Ni release from dNiTi material when implanted into the body. pNiTi remains at a greater risk of corrosion and Ni release in the body environment due to the increasing active surface and presence of secondary phases [12]. Of note, Ni-induced toxicity is of significant concern for pNiTi implants. As an immunotoxin and carcinogen, the accumulation of Ni and its compounds in the body through chronic exposure causes various adverse effects on human health. Based on Ni ion concentration and the exposure time, Ni-induced toxicity may be responsible for various human diseases, including contact dermatitis, allergy, cardiovascular disease, kidney disease, asthma, lung fibrosis, lung and nasal cancer [13].

Reports indicate that different fabrication parameters including green density, preheating temperature and heating rate affect the properties of synthesized alloy, including the strength and martensite transformation temperature [14–17]. The elastic modulus of pNiTi primarily depends on porosity [2], while the pore size has an impact on the electrochemical corrosion of pNiTi and corrosion resistance [18].

Despite these findings, studies on comparing Ni release and cytocompatibility between pNiTi and dNiTi have less been reported. In this study, the microstructure and metallurgical features of pNiTi produced by sintering evaporation method were investigated. Besides, Ni release and cytocompatibility between pNiTi and dNiTi alloys were compared.

## 2 Experimental

### 2.1 Material and specimen fabrication

The pNiTi samples were produced by sintering evaporation using Ti–50.8Ni (at.%) gas-atomized powders and NaCl space-holders. The particle size of Ti–Ni gas-atomized powders was less than 75  $\mu\text{m}$ . The particle size of NaCl space-holders was between 150 and 355  $\mu\text{m}$ . The mass ratio of Ti–Ni gas-atomized powders to NaCl space-holders was about 3:2. The powder mixture was vacuum hot

pressed at 780 °C for 4 h, with a pressure of 25 MPa and vacuum of  $1 \times 10^{-4}$  Pa, followed by sintering at 1050 °C for 4 h without pressure in the vacuum condition to evaporate the NaCl. The porosity of the porous NiTi alloy was  $(65 \pm 1.5)\%$ . The dNiTi samples were produced by the method reported in our previous study [11]. pNiTi and dNiTi used in this study have no surface treatment.

### 2.2 Material characterization

The morphological characteristics were observed by metallographic microscope and X-ray dispersive spectroscopy (XRD).

The porosity of the porous NiTi alloy is defined by

$$P = (1 - \rho / \rho_0) \times 100\% \quad (1)$$

where  $\rho$  is the density of pNiTi, calculated from the mass and theoretical volume, and  $\rho_0$  is the theoretical density of fully dense material ( $6.45 \text{ g/cm}^3$ ).

The structure of dNiTi alloy was investigated by X-ray diffraction (XRD) with Cu  $K_\alpha$  radiation on Dmax-2500 diffractometer.

### 2.3 In vivo and in vitro comparison of Ni release from pNiTi and dNiTi

Samples of pNiTi, dNiTi and Ti (as the control group, Ti medical implant purchased from Ningbo Cibe Company, China) were implanted into the thigh bones of the left hind leg of mice. Eight samples of each material type were separately implanted into 8 mice. The implanted materials were removed after 60 days. The *de novo* bone tissues on the surface of the samples were scanned, and then the amount of Ni in the fresh bone was analyzed under a Sirion 200 scanning electron microscope equipped with a GENESIS 60S energy dispersive spectroscope.

The evaluation of the difference of Ni release from pNiTi and dNiTi in vitro was based on the ISO 10993 for medical device biocompatibility Part 5. Samples of pNiTi, dNiTi and Ti were immersed in the simulated body fluid (SBF, 0.2 g/mL, pH 7.2) at 37 °C for 30 days under sterile conditions. Ni ion concentration in the extracting liquid was measured through dimethylglyoxime spectrophotometry (722N spectrophotometer, Shanghai Yidian, China). Each sample was replicated three times and the average values were recorded.

## 2.4 Comparison of cytocompatibility in pNiTi and dNiTi

The cytocompatibility of specimens was examined through a series of tests including cell proliferation, alkaline phosphatase (ALP) test and mitochondrial membrane potential assay. The extracting liquid of every kind of materials was re-used to culture preosteoblast MC3T3-E1 cells (bought from Shanghai Institute of Biochemistry and Cell Biology of Chinese Academy of Science). Experiments were undertaken in triplicate. Nine repeated tests were made for cell proliferation assay and ALP activity, while six repeated tests for apoptosis.

### (1) Cell culture

Preosteoblast MC3T3-E1 cells were cultured in the sterile extracting liquid with three kinds of materials on 96-well plates, containing penicillin (100 U/mL) and streptomycin (100 µg/mL) supplemented with 10% fetal bovine serum and kept at 37 °C in an atmosphere of 5% CO<sub>2</sub>.

### (2) Cell proliferation assay

For cell proliferation assay, preosteoblast MC3T3-E1 cells were cultured for 1, 3 and 7 days, respectively. After incubation, CCK8 enzyme-linked immunometric meter method (Cell Counting Kit-8, Dojindo, Japan) was performed following the manufacturer's instructions. Using the ELISA plate reader, the optical density (OD) value was recorded at 450 nm. The cell relative proliferation rate was calculated.

### (3) ALP activity test

ALP activity test was conducted to evaluate cell differentiation. After 1, 3, and 7 days, cells were lysed and assayed for their ALP activity using an alkaline phosphatase assay kit (A059-2-2, Nanjing Jiancheng, China).

### (4) Apoptosis test

The decrease of mitochondrial membrane depolarization (MMP) is a typical characterization at the early stage of apoptosis. The measurement of MMP was estimated using JC-1 dye (Mitochondrial membrane potential detection kit, C2006, Shanghai Biyuntian, China). Briefly, after being cultured for 1, 3 and 7 days, MC3T3-E1 cells were washed and incubated with JC-1 working solution for 20 min at 37 °C in the dark, washed with cold JC-1 staining buffer, placed on ice, and observed immediately by fluorescence microscopy.

## 2.5 Statistical analysis

Results were expressed as the mean±standard deviation on graphs. One-way ANOVA was used, followed by the Bonferroni test for post hoc analysis when multiple comparisons were conducted. Statistical analysis was performed using SPSS Graduate Park 19.0 software (SPSS, Inc., Chicago, IL, USA). A *P*-value of 0.05 or less ( $P \leq 0.05$ ) was considered statistically significant.

## 3 Results and discussion

### 3.1 Microstructure and mechanical property of pNiTi

pNiTi exhibits an irregular and interconnective pore structure closely similar with the human bone (Fig. 1(a)). The actual porosity of pNiTi is (65±1.5)%. The pore size is between 100 and 355 µm. The pore distribution is relatively uniform, and the pore morphology and size are similar to those of original NaCl. The XRD pattern of pNiTi is shown in Fig. 1(b). The main phases in the pNiTi alloy include TiNi (B2), TiNi (B19'), Ti<sub>2</sub>Ni and Ti<sub>3</sub>Ni<sub>4</sub>. The compression strength of pNiTi is about (125±3) MPa (Fig. 1(c)). The strength of fabricated pNiTi is higher than that of cancellous bone (1–100 MPa for human). The Young's modulus of the pNiTi alloy is measured to be (10.6±0.3) GPa, which is an intermediate value between cortical bone and cancellous bone [5,6]. Both porosity and pore size of pNiTi are correlated and crucial to the mechanical and biological properties, and may also determine the performance after implantation [2]. Porosity and pore size are two of key parameters that should be considered when pNiTi material is used for medical implant.

### 3.2 Ni release of pNiTi and dNiTi alloys

Samples of pNiTi and dNiTi were coated with *de novo* bone tissues after 60 days post-implantation in mice thigh bones. The quantity of Ni in the *de novo* bones was measured using a Sirion 200 scanning electron microscope equipped with a GENESIS 60S energy dispersive spectroscope (Fig. 2). The Ni contents in the newly formed bones on the surfaces of pNiTi materials ((1.95±0.87) wt.%; (0.47±0.21) at.%) are significantly higher than those on the surfaces of dNiTi materials ((0.62±0.19) wt.%; (0.15±0.05) at.%) ( $P < 0.05$ ). The results suggest the possibility of more Ni release

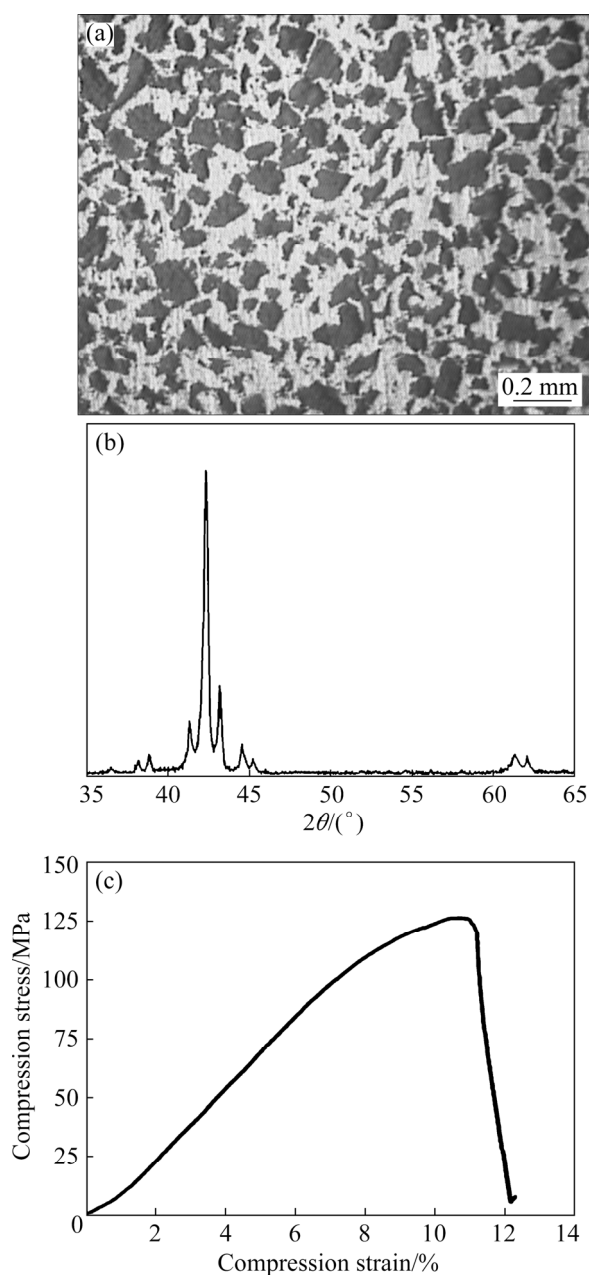


**Fig. 1** Microstructure and mechanical properties of pNiTi: (a) Microstructure; (b) XRD pattern; (c) Compression curve

from the pNiTi to the surrounding tissues than that from dNiTi if implanted in human bodies. Moreover, Ni release from pNiTi is much more than that from dNiTi samples in SBF (Fig. 3). Ni ion in the extracting liquid of pNiTi is  $(890.69 \pm 9.17) \mu\text{g/L}$ , whereas that of dNiTi is  $(346.46 \pm 8.92) \mu\text{g/L}$  ( $P < 0.001$ ).

XU et al [18] evaluated the impact of pore size on electrochemical corrosion of pNiTi in SBF and discovered that the corrosion resistance decreased with increasing pore size. Moreover, Ni releases

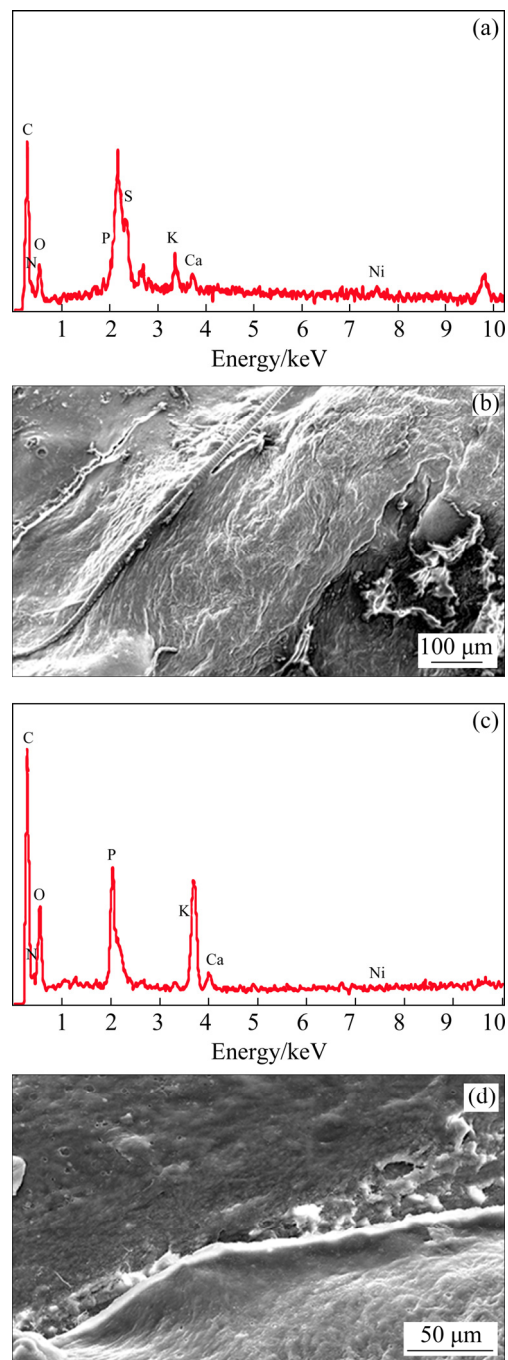


**Fig. 2** Ni release of pNiTi (a, b) and dNiTi (c, d) alloys

from the bare NiTi increased with exposure time, reaching a maximum value at 72 h, while that from TiN-coated NiTi alloy was kept at a significantly low level. Although cells proliferation on bare NiTi alloy within 72 h was similar to that on TiN-coated NiTi alloy, the expression of physiologically activity-related genes of cells on bare NiTi alloy was remarkably different from that on TiN-coated NiTi alloy [19,20], indicating that the released Ni from NiTi had a cytotoxic effect. Generally, pNiTi was reported to have a higher Ni release rate than

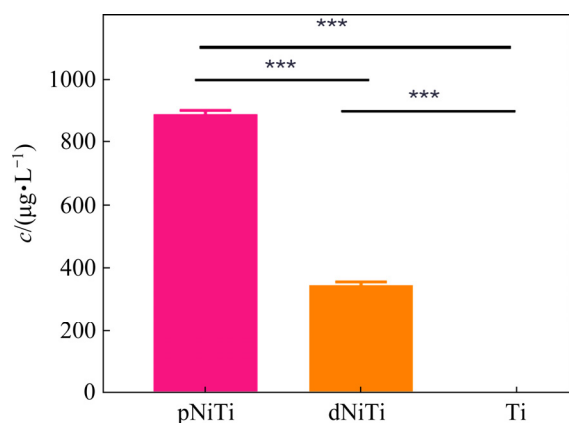


**Fig. 3** Concentration of Ni ions in extracting liquid of SBF (\*\* $P<0.001$ )

bulk dNiTi because of the increasing active surface and the presence of secondary phases [12]. Coating of hydroxyapatite bioactive ceramic particles on NiTi surfaces is a technique to prevent Ni release into the body [4]. SAADATI and AGHAJANI [9] reported that hydroxyapatite-coated pNiTi is also porous but with less corrosion resistance compared with pNiTi. This modified surface decreases the Ni release rate of NiTi implants in the SBF solution. This causes rapid absorption of additional proteins and promotes cell adhesion, and especially, osteoblasts potentially accelerate bone-implant chemical bond generation [9]. Besides designing appropriate porosity and pore size to decrease Ni release, surface of pNiTi implants should be treated or coated to improve the corrosion resistance.

### 3.3 Cytocompatibility of pNiTi and dNiTi

When MC3T3-E1 cells are cultured in different extracting liquid, a significant difference in cell proliferation is noted between the pNiTi and dNiTi groups on the 1st day, 3rd day, and 7th day ( $P<0.05$ ). By extending the cell culture time, the difference appears to expand. The cell relative proliferation rates of the pNiTi group on the 1st day, 3rd day and 7th day are  $(79.15\pm 12.26)\%$ ,  $(70.95\pm 7.15)\%$ , and  $(62.49\pm 4.54)\%$ , respectively (Fig. 4). Cells of the pNiTi group show lower ALP activity than that of the dNiTi group and control Ti group ( $P<0.05$ ) (Fig. 5). However, the difference in ALP activity between dNiTi alloy and Ti samples is nearly negligible. The ALP activity results show the effect of the implant material on the differentiation of preosteoblasts. A significant difference in cell differentiation is observed between the pNiTi and

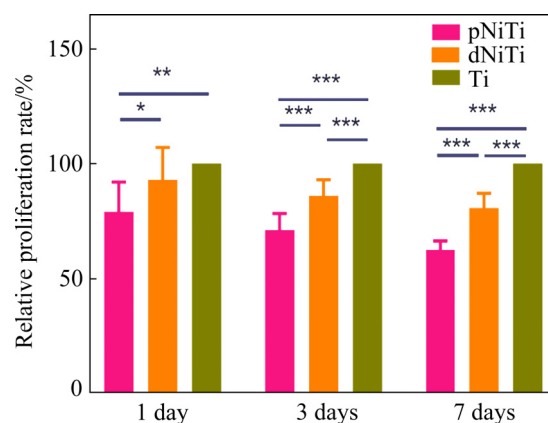


**Fig. 4** Relative proliferation rates of preosteoblast MC3T3-E1 cells of pNiTi, dNiTi and Ti group (\* $P<0.05$ ; \*\* $P<0.01$ ; \*\*\* $P<0.001$ )

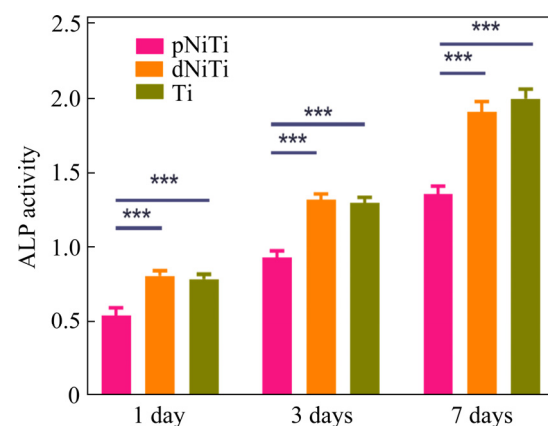


**Fig. 5** ALP activity of preosteoblast MC3T3-E1 cells of pNiTi, dNiTi and Ti group (\*\* $P<0.001$ )

dNiTi groups. This implies that pNiTi material inhibits cell differentiation.

The apoptosis of MC3T3-E1 cells in the pNiTi group is significantly increased compared to that in other groups (Fig. 6). SEVCIKOVA and PAVKOVA [20] suggested that the evaluation of implant materials should not be based only on cell proliferation; instead, other aspects including cell morphology, cellular expression and apoptosis should also be considered. Notably, cytotoxicity is an essential evaluation parameter of the cytocompatibility of biomaterials. Cytotoxicity of pNiTi alloy is a challenge for medical use unless the material is surface treated or coated.

Studies on the biocompatibility of NiTi have largely matured in the past decades [21,22]. NiTi represents efficient in vitro cell compatibility and in vivo biocompatibility [23]. The relationship between the biocompatibility of NiTi and Ni release remains controversial. Although excessive Ni ion

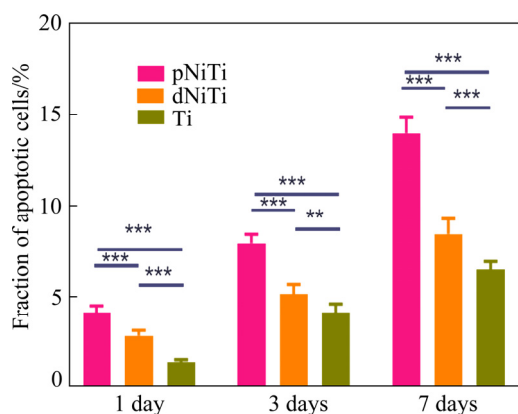


**Fig. 6** Apoptosis of preosteoblast MC3T3-E1 cells cultured in extracting liquid of pNiTi, dNiTi and Ti samples (\*\* $P < 0.01$ ; \*\*\* $P < 0.001$ )

causes toxicity, allergic reaction and cancer [13], some scholars believe that the release level of Ni ions from NiTi is well tolerated [24] and the amount of released Ni is too low to have an impact on cytocompatibility [25]. In our experiment, we examined the effects of pNiTi, dNiTi and Ti extracting liquid on preosteoblast cell proliferation, differentiation, and apoptosis. A significant difference is noted among the three groups, specifically pNiTi which demonstrates impaired impact on cell bioactivity. This poses a significant concern for the safety of pNiTi in clinical use. Further studies are necessary to comprehensively understand the relationship between the biocompatibility of NiTi and Ni ion.

## 4 Conclusions

(1) pNiTi prepared by sintering evaporation method is mechanically similar to bone.

(2) Ni releases from the uncoated pNiTi in vivo or in vitro are more serious than those from dNiTi.

(3) There is a significant difference in cytocompatibility between pNiTi and dNiTi. pNiTi significantly interferes with the proliferation and differentiation of bone cells, causing early apoptosis. Thus, a significantly cautious approach should be adopted when using it as a medical implant.

## References

[1] BHARDWAJ A, GUPTA A K, PADISALA S K, POLURI K. Characterization of mechanical and microstructural

properties of constrained groove pressed nitinol shape memory alloy for biomedical applications [J]. *Materials Science and Engineering C: Materials for Biological Applications*, 2019, 102: 730–742.

[2] HABIJAN T, HABERLAND C, MEIER H, FRENZEL J, WITTSIEPE J, WUWER C, GREULICH C, SCHILDHAUER T A, KOLLER M. The biocompatibility of dense and porous nickel–titanium produced by selective laser melting [J]. *Materials Science and Engineering C: Materials for Biological Applications*, 2013, 33(1): 419–426.

[3] WANG Xie-bin, KUSTOV S, Van HUMBEECK J. A short review on the microstructure, transformation behavior and functional properties of NiTi shape memory alloys fabricated by selective laser melting [J]. *Materials (Basel, Switzerland)*, 2018, 11(9): 1683.

[4] KHALILI V, KHALIL-ALLAFI J, SENGSTOCK C, MOTEMANI Y, PAULSEN A, FRENZEL J, EGGELER G, KOLLER M. Characterization of mechanical properties of hydroxyapatite–silicon–multi-walled carbon nano tubes composite coatings synthesized by EPD on NiTi alloys for biomedical application [J]. *Journal of the Mechanical Behavior of Biomedical Materials*, 2016, 59: 337–352.

[5] BASSANI P, PANSERI S, RUFFINI A, MONTESI M, GHETTI M, ZANOTTI C, TAMPIERI A, TUISSI A. Porous NiTi shape memory alloys produced by SHS: Microstructure and biocompatibility in comparison with  $Ti_2Ni$  and  $TiNi_3$  [J]. *Journal of Materials Science: Materials in Medicine*, 2014, 25(10): 2277–2285.

[6] ZYSSET P K, GUO X E, HOFFLER C E, MOORE K E, GOLDSTEIN S A. Elastic modulus and hardness of cortical and trabecular bone lamellae measured by nanoindentation in the human femur [J]. *Journal of Biomechanics*, 1999, 32(10): 1005–1012.

[7] LAI Tao, XU Ji-lin, XIAO Qi-fei, TONG Yun-xiang, HUANG Jun, ZHANG Jian-ping, LUO Jun-ming, LIU Yong. Preparation and characterization of porous NiTi alloys synthesized by microwave sintering using Mg space holder [J]. *Transactions of Nonferrous Metals Society of China*, 2021, 31(2): 485–498.

[8] AIHARA H, ZIDER J, FANTON G, DUERIG T. Combustion synthesis porous nitinol for biomedical applications [J]. *International Journal of Biomaterials*, 2019, 2019: 4307461.

[9] SAADATI A, AGHAJANI H. Fabrication of porous NiTi biomedical alloy by SHS method [J]. *Journal of Materials Science: Materials in Medicine*, 2019, 30(8): 92.

[10] BANSIDDHI A, SARGEANT T D, STUPP S I, DUNAND D C. Porous NiTi for bone implants: A review [J]. *Acta Biomaterialia*, 2008, 4(4): 773–782.

[11] YANG Shu, ZHOU Fei, XIAO Tao, XU Da-bao, LI Zhou, XIAO Zhu, XIAO Z A. Surface modification with  $SiO_2$  coating on biomedical TiNi shape memory alloy by sol–gel method [J]. *Transactions of Nonferrous Metals Society of China*, 2015, 25(11): 3723–3728.

[12] ELIAZ N. Corrosion of metallic biomaterials: A review [J]. *Materials (Basel, Switzerland)*, 2019, 12(3): 407.

[13] GENCHI G, CAROCCI A, LAURIA G, SINICROPI M S, CATALANO A. Nickel: Human health and environmental toxicology [J]. *International Journal of Environmental*

- Research and Public Health, 2020, 17(3): 679.
- [14] TOSUN G, ORHAN N, ÖZLER L. Investigation of combustion channel in fabrication of porous NiTi alloy implants by SHS [J]. *Materials Letters*, 2012, 66(1): 138–140.
- [15] KAYA M, ORHAN N, TOSUN G. The effect of the combustion channels on the compressive strength of porous NiTi shape memory alloy fabricated by SHS as implant material [J]. *Current Opinion in Solid State and Materials Science*, 2010, 14(1): 21–25.
- [16] HU L, JIANG S Y, SHI L X, ZHANG Y Q. Prediction of grain scale plasticity of NiTi shape memory alloy based on crystal plasticity finite element method [J]. *Transactions of Nonferrous Metals Society of China*, 2019, 29(4): 775–784.
- [17] SHARIFI E M, KERMANPUR A. Superelastic properties of nanocrystalline NiTi shape memory alloy produced by thermomechanical processing [J]. *Transactions of Nonferrous Metals Society of China*, 2018, 28(3): 515–523.
- [18] XU J L, BAO L Z, LIU A H, JIN X J, TONG Y X, LUO J M, ZHONG Z C, ZHENG Y F. Microstructure, mechanical properties and superelasticity of biomedical porous NiTi alloy prepared by microwave sintering [J]. *Materials Science and Engineering C: Materials for Biological Applications*, 2015, 46: 387–393.
- [19] ZHAO L F, HONG Y, YANG D Y, LV X Y, XI T F, ZHANG D Y, HONG Y, YUAN J F. The underlying biological mechanisms of biocompatibility differences between bare and TiN-coated NiTi alloys [J]. *Biomedical Materials (Bristol, England)*, 2011, 6(2): 25012.
- [20] SEVCIKOVA J, PAVKOVA G M. Biocompatibility of NiTi alloys in the cell behaviour [J]. *Biometals*, 2017, 30(2): 163–169.
- [21] DENG Bi-wei, BRUZZANITI A, CHENG G J. Enhancement of osteoblast activity on nanostructured NiTi/hydroxyapatite coatings on additive manufactured NiTi metal implants by nanosecond pulsed laser sintering [J]. *International Journal of Nanomedicine*, 2018, 13: 8217–8230.
- [22] TATESHIMA S, KANEKO N, YAMADA M, DUCKWILER G, VINUELA F, OGAWA T. Increased affinity of endothelial cells to NiTi using ultraviolet irradiation: An in vitro study [J]. *Journal of Biomedical Materials Research: Part A*, 2018, 106(4): 1034–1038.
- [23] ES-SOUNI M, ES-SOUNI M, FISCHER-BRANDIES H. Assessing the biocompatibility of NiTi shape memory alloys used for medical applications [J]. *Analytical and Bioanalytical Chemistry*, 2005, 381(3): 557–567.
- [24] HANG R, LIU Y, LIU S, BAI L, GAO A, ZHANG X, HUANG X, TANG B, CHU P K. Size-dependent corrosion behavior and cytocompatibility of Ni–Ti–O nanotubes prepared by anodization of biomedical NiTi alloy [J]. *Corrosion Science*, 2016, 103: 173–180.
- [25] HANG Rui-qiang, LIU Yan-lian, LIU Si, BAI Long, GAO Ang, ZHANG Xiang-yu, HUANG Xiao-bo, TANG Bin, CHU P K. Relationship between Ni release and cytocompatibility of Ni–Ti–O nanotubes prepared on biomedical NiTi alloy [J]. *Corrosion Science*, 2017, 123: 209–216.

## 多孔与致密镍钛合金的镍释放及细胞相容性比较

余本铨<sup>1</sup>, 袁文慧<sup>1</sup>, 徐强<sup>2</sup>, 古韵芳子<sup>1</sup>, 肖明明<sup>1</sup>, 徐国富<sup>2</sup>, 李周<sup>2</sup>, 肖柱<sup>2</sup>, 肖自安<sup>1</sup>

1. 中南大学 湘雅二医院耳鼻咽喉头颈外科, 长沙 410011;

2. 中南大学 材料科学与工程学院, 长沙 410083

**摘要:** 采用蒸发烧结法将 Ti–50.8Ni(摩尔分数, %)气体雾化粉末制备成多孔镍钛合金(pNiTi)样品, 采用金相显微镜和 X 射线衍射仪(XRD)对样品进行分析, 并比较 pNiTi 和致密 NiTi(dNiTi)的镍释放和细胞相容性。结果表明, pNiTi 具有良好的力学性能。在体内外, pNiTi 的镍释放较 dNiTi 严重。用 pNiTi 浸提液培养的细胞增殖和分化较弱, 早期凋亡率较高。综上所述, pNiTi 在力学上与骨相似, 但释放的 Ni 会干扰骨细胞的增殖和分化。使用 pNiTi 作为医疗植入物应进行谨慎处理。

**关键词:** 多孔镍钛合金; 力学性能; 镍释放; 细胞相容性

(Edited by Bing YANG)